

Characterization of the Mechanical Behavior and Fatigue Property for Ti Films by Nanoscale Dynamic-Mechanical-Analysis

Liu Jinna^{1,2}, Wang Haidou², Xing Zhiguo², Xu Binshi², Cui Xiufang¹, Jin Guo¹

¹ Harbin Engineering University, Harbin 150001, China; ² National Key Laboratory for Remanufacturing, Academy of Armored Forces Engineering, Beijing 100072, China

Abstract: The mechanical behavior and the fatigue property of Ti films with different thickness were investigated by nanoindentation test. The fatigue property of the films was quantitatively calculated according to the changes of storage stiffness based on the nanoscale dynamic mechanical analysis. The results show that the fatigue life of the films depends on the residual stress remarkably. In situ scanning images show the thin film is significantly stacked and layered, and the long cracks radiate from the center of the indenter perpendicular to the indenter edge. Additionally, there is a sizable stress pile up around the indentations which demonstrate that a highly localized plastic deformation and stress release occurs in the process of the nanoscale dynamic loading process. The existence of the internal compressive residual stress will offset part of the load stress to improve the fatigue life of films.

Key words: Ti film; fatigue; nanoindentation; nanoscale dynamic-mechanical-analysis; residual stress

Film-substrate materials have been extensively used in micro-electronic mechanical system (MEMS) and information science and technology areas because of their unique structure and properties. MEMS thin film materials are generally of micron size to nanoscale, together with their complex service environments. The scale, interface and heterogeneous constraint effects are very obvious^[1,2]. It is extremely difficult to fully describe the mechanical properties and damage mechanism of material performance characterization by the classical macroscopic continuum and microscopic quantum theory^[3,4]. Nowadays, characterization methods for film mechanical properties include the uniaxial tension method, nanoindentation method, bubbling method, and micro-beam bending method, etc^[5]. Hommel et al^[6] prepared metallic Cu film on a polymer substrate which has high flexibility. Loop loading on the polymer substrate achieved cyclic tension-compression loading of the thin metal film. This method can

be employed to fatigue testing of the film in sub-micron thickness, but the actual cyclic plastic strain amplitude during the fatigue loading cannot be determined. Micro-cantilever beam specimens with Ag film and SiO₂ substrate were prepared by Schwaiger^[7]. A continuous stiffness measurement system provided dynamic bending load on them. Continuous stiffness values decreased continuously with the fatigue test, and the cracks appeared during the test. The stress-strain relationship of the plastic deformation zone is relatively intricate, making a quantitative calculation very difficult^[8].

Nanoindentation test technology can test a variety of thin film surface mechanical properties due to a high resolution of the load and displacement. It is multi-functional micro/nano mechanics measuring probe which can determine the hardness, elastic modulus, fracture toughness, and fatigue^[9-12]. In the previous studies, our team tried to test the fatigue performance of 20, 100, and 1000 nm thick Cu films by using the

Received date: June 13, 2019

Foundation item: National Natural Science Foundation of China (51535011, 51705095, 51775554); National Basic Research Program of China ("973" Program) (61328303); Postdoctoral Scientific Research Developmental Fund of Heilongjiang Province (LBH-Q18036); Natural Science Foundation of Heilongjiang Province (LH2019E031); Fundamental Research Funds for the Central Universities (HEUCF)

Corresponding author: Wang Haidou, Ph. D., Professor, National Key Laboratory for Remanufacturing, Academy of Armored Forces Engineering, Beijing 100072, P. R. China, Tel: 0086-10-66718541, E-mail: wanghaidou@aliyun.com

Copyright © 2020, Northwest Institute for Nonferrous Metal Research. Published by Science Press. All rights reserved.

nanindentation test. But we only obtained the fatigue life of the 20 nm thick film under a mean load of 1 mN^[13]. The fatigue life for the thicker films of 100 and 1000 nm thick cannot be measured. After times trying, when the size of the average load went down to μN level, the fatigue life could be measured for a thicker film and the test results were obvious.

The mechanical properties of thin film materials determine the reliability and service life of the film. In order to determine the performance of film materials by nanoscale mechanical testing methods, and research the effects of residual stress on the mechanical properties of the films, nanoscale Ti films were prepared by using a magnetron sputtering system. The Ti metal crystal structure belongs to the hexagonal crystal system. Titanium and its alloy have the advantages of high strength. They are generic MEMS materials which have been widely used in conduct electricity. The film which is thin enough shows an observable small size effect and a better performance than a thick film. In addition, the mechanical properties are also influenced by a different substrate. In this paper, 100 and 400 nm thick Ti films were prepared on both monocrystalline silicon and glass substrate using the magnetron sputtering. The nanoscale mechanics tester was used to measure the micro-mechanical properties of the films. The growth mechanism of the thin film on different substrates and the film fatigue damage failure mechanism were discussed.

1 Experiment

The 100 and 400 nm thick Ti films were deposited on one-side-polished single crystal Si<100> and glass substrates by DC magnetron sputtering method. The sputtering material dimension was $\Phi 80$ mm and 6 mm thick, and Ti target purity is 99.99%. Before sputtering started, the target material needed pre-sputtering for 15 min to eliminate the surface oxide layer. Then the substrate materials were cleaned using high purity acetone and then washed by Ar ion for 10 min. Vacuum of the magnetron sputtering cavity bottom was 1.33×10^{-3} Pa, the work pressure was 0.667 Pa, the gas flow rate was 3.38×10^{-2} m³/s, work power was 150 W, and the sputtering rate was 20 nm/min.

Atomic force microscope (AFM) was used to observe film surface morphology and roughness, and transmission electron microscopy (TEM) was used to analyze the thin film microstructure. The three-dimensional stress distribution of the thin film was measured by a film electronic stress distribution tester (GS6341). The measuring principle was based on the changes in the curvature radius of the substrate before and after sputtering, and the Stoney equation (1) was used to calculate the film stress value:

$$\sigma(x, y) = \frac{E d_s^2}{6(1-\nu) d_f} \cdot \frac{1}{R(x, y)} \quad (1)$$

where E and ν are Young's modulus and Poisson's ratio of the

substrate, respectively; d_s and d_f are the thickness of Si substrate and the film, respectively; $R(x, y)$ is the curvature radius of the substrate at the point (x, y) . When $\sigma > 0$, it is tensile stress, while $\sigma < 0$ is compressive stress.

The dynamic contact module (DCM) of Agilent G200 type nano-indentation apparatus was used to monitor continuous stiffness measurement (CSM) for acquiring modulus and nanohardness values. This method has the advantage of improving the resolution of the load and the displacement at the same time and reduces the sensitivity to environmental noise. Even at a depth of only 10 nm, it can guarantee the accuracy of the actual measurement results. So, it was more reliable.

The dynamic mechanics analysis (DMA) module of TriboIndenter low-load situ nonmechanical system was used to carry out the nanoscale film fatigue test. Storage modulus, loss modulus and phase-angle were obtained from samples under different frequencies and loads in the DMA test. The degree of contact stiffness was deduced. The contact stiffness was sensitive to damage deformation, so it could be used to determine the degree of fatigue damage:

$$E' = \frac{k_s \sqrt{\pi}}{2\sqrt{A_c}} \quad (2)$$

$$E'' = \frac{\omega C_s \sqrt{\pi}}{2\sqrt{A_c}} \quad (3)$$

where E' is the storage modulus; E'' is the loss modulus; k_s is the stiffness; C_s is the damping size; ω is the input frequency; and A_c is the contact area.

2 Results and Discussion

2.1 Surface topography and roughness

Fig.1 shows the surface morphology of the films measured by AFM (atomic force microscope). Island-like particles of similar size are evenly distributed on the surface of the film. The vertical growth trend of the particles becomes apparent with the increase of film thickness. This is mainly caused by self-shadowing because the sputtered metal films usually develops a columnar structure with a crystal phase. For the Ti film on Si substrate, the maximum height of the surface particles increases from 7 nm to 27 nm as the film thickness changes from 100 nm to 400 nm. The roughness of the film surface also increases with film thickness increasing gradually. The root mean square roughness (R_{ms}) of the thin films are shown in Table 1. The roughness of Ti films on the glass substrate is smaller than on the Si substrate.

2.2 Structure and crystallographic orientation

Fig.2 shows the high-resolution transmission electron micrograph (HRTEM) images and selected-area electron diffraction (SAED) pattern of Ti films. Small-sized grains are evenly distributed within the films. The grain boundary is obvious and grain size enlarges with the increasing of sputtering time for the Ti film on Si substrate. The grain size of Ti films on the glass substrate is larger than on the Si substrate. Additionally,

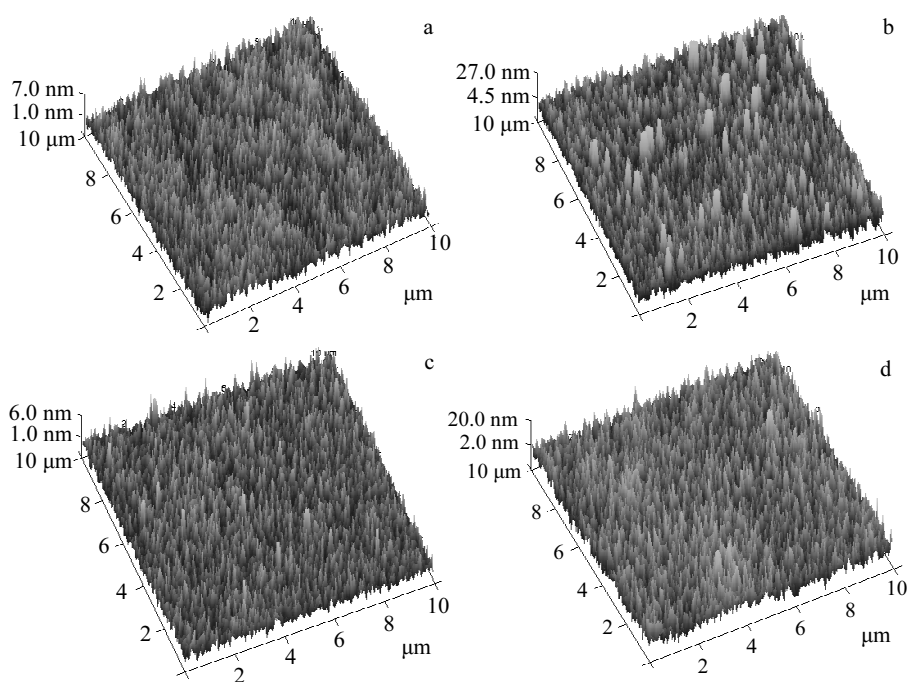


Fig.1 AFM characterization of Ti films with different thicknesses and substrates: (a) 100 nm thick with Si substrate (100-Si); (b) 400 nm thick with Si substrate (400-Si); (c) 100 nm thick with glass substrate (100-G); (d) 400 nm thick with Glass substrate (400-G)

Table 1 Roughness of the Ti films

Ti film	100-Si	400-Si	100-G	400-G
Roughness/nm	1.48	4.44	1.14	4.19

the grains size increases with the increasing of film thickness. When the film thickness reaches 400 nm, the inner structure of

the thin film appears like a cloud with no obvious grains and grain boundary.

The Ti film crystal structure on the Si substrate is significantly different from on the glass substrate, as shown by the diffraction patterns. The Ti film on the Si substrate shows a typical hexagonal close-packed (hcp) structure and obvious

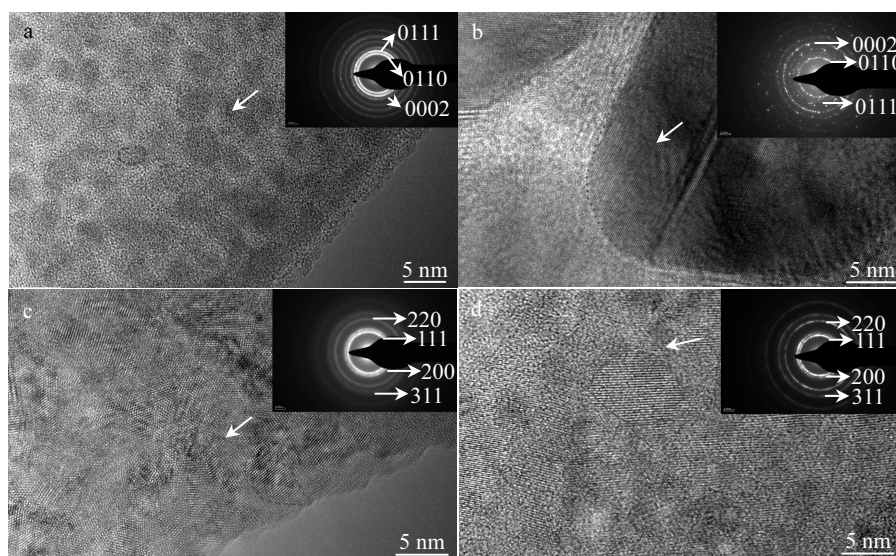


Fig.2 HRTEM images of Ti films with different thicknesses and substrates: (a) 100-Si, (b) 400-Si, (c) 100-G, and (d) 400-G (insets in the upper-right corner are corresponding selected-area electron diffraction patterns)

orientation (0110) while the face-centered cubic structure of the Ti film on the glass substrate shows a strong (111) preferred orientation. The lattice spacing is about 0.2 nm for the four kinds of film. The results are similar to previous research^[14,15]. During the magnetron sputtering process, the formation of Ti ions from the bombardment of Ti particles produces many crystal nuclei for thin film deposition of nanometer grain film with a uniform-sized particle distribution. However, Ti metallic bond has no direction and saturation. The glass substrate has no crystal orientation, which is distinct from the single crystal silicon substrate, so it is not easy to crystallize. The growth of thin films tends to a more closely packed arrangement. The fcc structure is the most closely packed crystal structure which forms in the Ti nanocrystalline films on the glass substrate.

2.3 Nanohardness and modulus

Fig.3 shows the nanohardness-displacement curves (Fig.3a) and the modulus-displacement curves (Fig.3b) of films measured by continuous stiffness measurement. The test depth was 400 nm. The film hardness and modulus values are shown in Table 2. The testing process of nano-hardness is divided into three stages: the first stage is the indentation size effect stage, corresponding prior to the point A on the curve. The thin film material is at the elastic stage under the indenter. Because of the indentation size effect, the nanohardness of the film increases gradually. When the depth is between A and B, the thin film material is still in the elastic deformation stage, but the nanohardness value changes slowly. The indentation

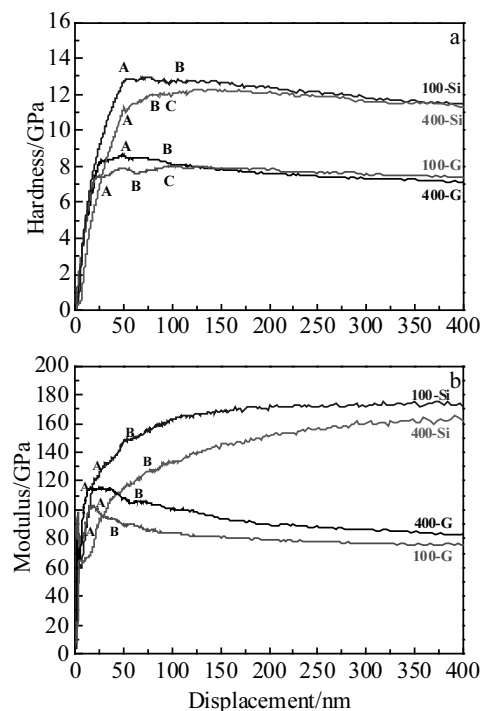


Fig.3 Relation curves of hardness (a) and modulus (b) versus displacement for Ti films

Table 2 Hardness and modulus values of the Ti films

Ti films	100-Si	400-Si	100-G	400-G
Hardness/GPa	9.8	7.3	8.3	7.4
Modulus/GPa	121	114	96	109

size effect weakens and the nanohardness value is measured at this stage. When the depth is greater than point B, the plastic deformation of the thin film continues. The influence of substrate increases with the increase of indentation depth. The measured nanohardness value of the thin film approaches that of the substrate. The hardness value changes when the depth reaches the interface of the film and substrate (shown as point C).

2.4 Fatigue tests

Fig.4 shows the storage stiffness-time curves of Ti films tested by the nanoscale mechanical analysis module. The range of quasi-static loading was 1~100 μN , the dynamic load amplitude was 1.5 μN and loading rate was 25 $\mu\text{N/s}$. The frequency was 45 Hz and testing time was 200 s. The number of total cycles was 0.9×10^4 . Contact stiffness is the deformation resistance ability of the material's surface under the external force which is sensitive to damage deformation. In this way, the study of fatigue behavior by measuring the changes of the contact stiffness was carried out^[16].

The storage stiffness value of the 100 nm thick Ti film on Si substrate in the initial stage basically vibrates in a smaller range and maintains a value of 12.7 $\mu\text{N/nm}$. When testing reaches 121 s, total cyclic number is 0.54×10^4 , the stiffness suddenly falls to 10.9 $\mu\text{N/nm}$ and the film begins to undergo fatigue failure. The number of cycles N_f is defined as the fatigue life in which failure occurs. The stiffness value continues to fall sharply with the increasing of load cycle. When film fatigue failure occurs, the size of energy loss due to plastic deformation is no longer falling. For the 400 nm thick Ti film on Si substrate, the storage stiffness value at the initial stage fluctuates within a small range. The thin film deformation is mainly composed of elastic deformation accompanied by partial plastic deformation. When loaded to 138 s, the storage stiffness value suddenly falls: the film fatigue damage occurs. The fatigue life is 0.62×10^4 . And the fatigue lives of 100 and 400 nm thick films on the glass substrate are 0.53×10^4 and 0.59×10^4 , respectively.

Fig.5 is the fatigue damage morphologies of Ti films. Obvious fatigue failure occurs in all the Ti films with crack, delamination and spalling. Around the indentation, the thin film is stacked and layered. Long cracks radiates from the center of the indenter perpendicular to the indenter edge. The effect of the substrate on the fatigue life is not significant. However, the thinner the film is, the more serious the peeling is.

In the previous study, three stages appear to exist in the indentation fatigue damage: the indentation-induced by compression; the delamination and buckling; and the crack formation at the edge of the indentation. In the second stage, buckling occurs

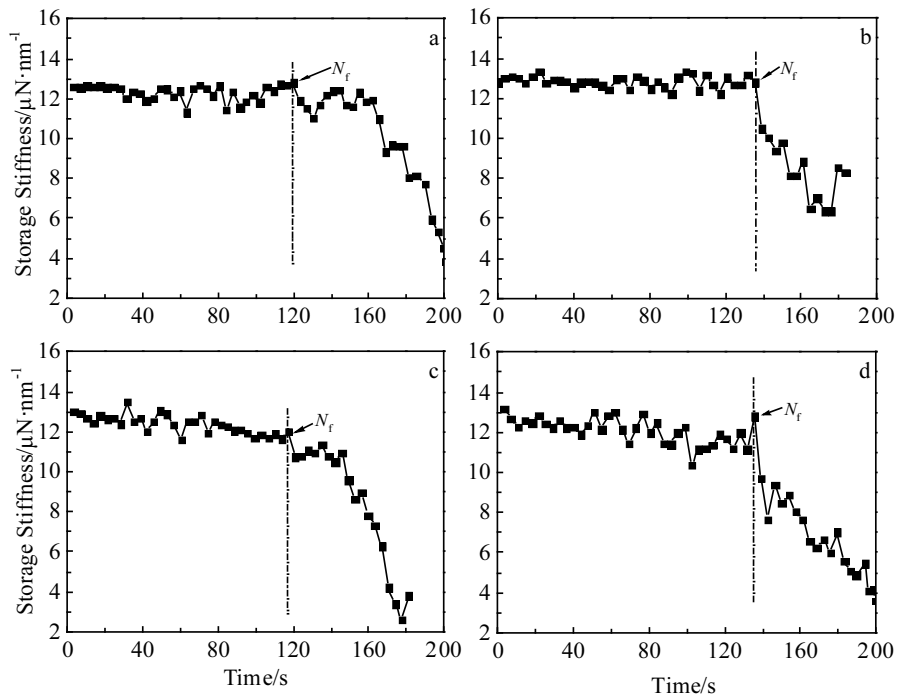


Fig.4 Storage stiffness-time curves of Ti films with different thicknesses and substrates: (a) 100-Si, (b) 400-Si, (c) 100-G, and (d) 400-G

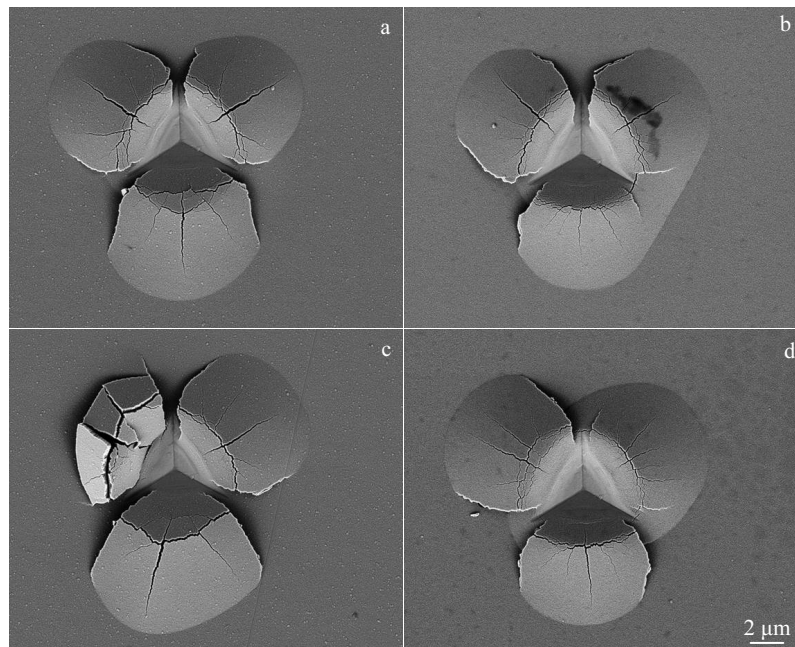


Fig.5 Fatigue failure morphologies of Ti films with different thicknesses and substrates: (a) 100-Si, (b) 400-Si, (c) 100-G, and (d) 400-G

during the unloading segment of fatigue testing cycle when the sum of indentation compressive stress σ_i and the residual stress σ_r exceeds the critical buckling stress σ_b for the delaminated circular section as given by:

$$\sigma_b = \frac{\mu^2 E}{12(1-\nu^2)} \left(\frac{t}{a} \right)^2 \quad (4)$$

where ν and E are the Poisson's ratio and elastic modulus of

the film, respectively; a is the crack radius, t is the film thickness, and μ is a constant.

The buckling film serves as a cantilever. Then, the indenter indents a cantilever rather than a film/substrate system with a much less contact stiffness. Therefore, the contact stiffness shows an abrupt decrease at the N_f . In the third stage, the delaminated and buckled size increases with increasing the number of cycles, resulting in a further decrease in contact stiffness since the cantilever beam length increases^[17]. Fatigue damage starts with the interfacial crack initiation and propagation. Compressive residual stresses promote delamination and buckling. So, high film bonding strength and proper residual stress are necessary for a higher fatigue life of the films.

2.5 Effects of residual stress and bonding strength on the fatigue properties of Ti films

The three-dimensional stress distribution of the films was measured by the electronic film stress testing system. A $\Phi 44.5$ mm homogeneous area is selected, shown in Fig.6. The maximum stress S_{\max} , minimum stress S_{\min} and average stress value S_{avg} are shown in Table 3. The average stress values are all characterized as residual compressive stress. Ti film compressive residual stress decreases with the increase of film thickness. Therefore, the distribution of stress gradually

becomes more uniform. The stress value decreases from 0.184 GPa to 0.021 GPa as the Ti film thickness increases from 100 nm to 400 nm on glass substrate. Compared to the Ti film on the glass substrates, Ti films on Si substrate have larger stress values.

The principle of magnetron sputtering is based on the action of Ar ion bombardment. The film and substrate are inclined to form intrinsic compressive stress, so that each film is characterized as compressive stress in this experiment. The thermal expansion coefficient of Ti film is greater than those of the single crystal silicon ($4.8 \times 10^{-8}/^\circ\text{C}$) and the glass ($5.5 \times 10^{-7}/^\circ\text{C}$). So Ti films on Si substrate have a greater thermal tensile stress. Compared to the massive materials, the grain's specific surface area of the thin film is larger. The tensile stress increases with the increasing of film thickness due to grain boundary diffusion, defects decrease in amount, and the specific surface area of crystal grain decreases, too.

When the dynamic loads are carried on, the internal compressive residual stress offset part of the load stress to improve its fatigue life. Smaller surface roughness in a thinner film reduces the incentives for surface crack initiation. Then, the higher surface residual compressive stress may hinder crack initiation at the film surface. It would be squeezed into the internal weak area which has the residual tensile stress. When

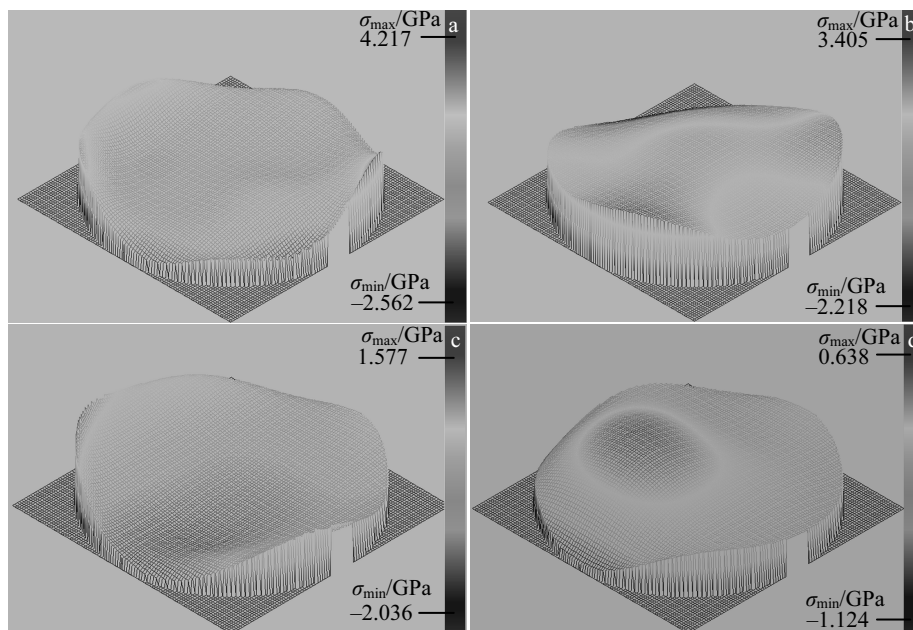


Fig.6 Three-dimensional stress distribution of the Ti films with different thicknesses and substrates: (a) 100-Si, (b) 400-Si, (c) 100-G, and (d) 400-G

Table 3 Stress distribution of the Ti films (GPa)

Ti film	100-Si	400-Si	100-G	400-G
σ_{\max}	4.217	3.405	1.577	0.638
σ_{\min}	-2.562	-2.218	-2.036	-1.124
σ_{avg}	-0.258	-0.182	-0.184	-0.021

the internal crack initiates, the local load stress is reduced and the dislocation slip is restrained. The local resistance is improved and the surface fatigue strength is improved^[18,19].

Fig.7 shows the scratch depth-displacement curves under the maximum load 10 mN by the nano-scratches method. The

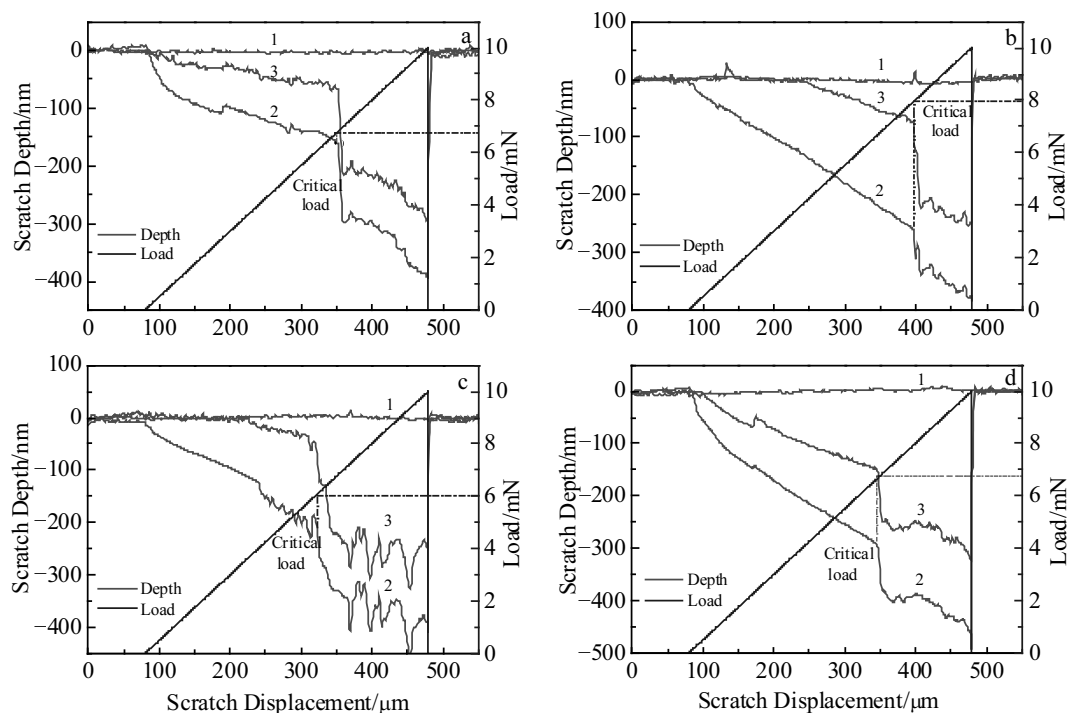


Fig.7 Scratch depth-displacement curves of the Ti films with different thicknesses and substrates: (a) 100-Si, (b) 400-Si, (c) 100-G, and (d) 400-G

whole process is divided into three stages: the preliminary-scanning, carved-scanning and after-scanning. In the carved-scanning (the curve signed 2 in the Fig.7), the vertical load increases from 20 μN to 10 mN within 400 μm displacements. The initial stage, scratched depth linearly increases almost with no mutation, and film peeling does not happen at this stage. The curves begins to fluctuate and shows a sharp decline when depth reaches 160, 290, 200, and 310 nm for the 4 kinds of films, respectively. Then the film starts peeling or cracking. Define the critical load as the needed minimum load under which continuous stripping of the thin film from the substrate by the indenter completely penetrates on the film. The size of the critical load value could reflect the bond strength of the thin film and substrate. The bond strengths of 100 and 400 nm thick films on Si substrates are 6.8 and 7.9 mN, respectively. The bond strength of 100 and 400 nm thick films on glass substrates are 6.1 and 6.8 mN, respectively. After-scanning stage is mainly used to get the surface information of scratches damage, and to gain the elastic recovery state by contrast with the pre-scanning curve and carved scanning curve. So, the elastic recovery of the Ti film on the glass substrate is better than on the Si substrate.

Bond strength of the thin film and substrate is related to the intrinsic material properties of the thin film and substrate, the film thickness, surface roughness and hardness of the substrate, residual stresses in the thin film and some other factors. When the films have the same thickness, the higher hardness of the

substrate produces the stronger supporting function from the substrate. The Ti film and Si substrate are typical soft film/hard substrate structure, and Ti-film and glass substrate are hard film/soft substrate structure. When the films thicknesses are the same, the bond strength of Ti film on the Si substrate is greater. The existence of the residual stress in the film will weaken the bond strength between the film and substrate, and the film is easy to dehiscence and peeling up to shorten the service life^[20,21]. In addition, the bigger the substrate surface roughness is (during a regular range), the greater the bond strength of the film and the substrate is. The initial surface roughness of monocrystalline silicon and the glass substrate are 1.26 and 7.02 nm, respectively. So, the bond strength of Ti film on the glass substrate should be larger when the film thickness is the same. And the final size of the bond strength is a combined result of several factors in the front. Comprehensively, the bond strength of Ti film on Si substrate is greater. This is helpful to improve its fatigue life.

3 Conclusions

1) Surface roughness increases with increasing the film thickness. The Ti film on the Si substrate is the typical hcp structure with obvious orientation (0110). The Ti film on the glass substrate is the fcc structure with a strong (111) preferred orientation.

2) There are compressive residual stresses in the four kinds of film, and when the film thickness is thinner, the

compressive residual stresses in it would be larger.

3) Internal residual compressive stress in the film will suppress the fatigue crack initiation, and then improve the fatigue life of the film.

References

- 1 Cao Xiankun, Shao Tianmin, Wen Shizhu et al. *Tribology Transactions*[J], 2004, 47(2): 227
- 2 Yu Yi, Ren Tianling, Liu Litian. *Integrated Ferroelectrics*[J], 2005, 69(1): 367
- 3 Campanelli LC, Duarte L T, Paulo Sergio Carvalho Pereira da Silva et al. *Materials and Design*[J], 2014, 64: 393
- 4 Skordaris G. *Journal of Materials Engineering and Performance* [J], 2014, 23: 3497
- 5 Mei-ling Lau, Kin-tak Lau, Yan-dong Yao Yeo et al. *Materials and Manufacturing Processes*[J], 2010, 25(5): 324
- 6 Hommel M, Kraft O, Arzt E. *Journal of Materials Research*[J], 1999, 14 (6): 2373
- 7 Schwaiger R, Kraft O. *Scripta Materialia*[J], 1999, 41(8): 823
- 8 Zhang G P, Schwaiger R, Volkert C A. *Philosophical Magazine Letters*[J], 2003, 83(8): 477
- 9 Zong Z, Lou J, Adewoye O O et al. *Materials Science and Engineering A*[J], 2006, 434:178
- 10 Lu Chunpeng, Gao Hang, Wang Jinghe et al. *Materials and Manufacturing Processes*[J], 2010, 25(8): 740
- 11 Beake B D, Fox-Rabinovich G S, Veldhuis S C et al. *Surface & Coatings Technology*[J], 2009, 203: 1919
- 12 Li Xiaodong, Bhushan Bharat. *Scripta Materialia*[J], 2002, 47: 473
- 13 Liu J N, Xu B S, Wang H D et al. *Materials & Design*[J], 2015, 65: 1136
- 14 Chen A Y, Bu Y, Tang Y T et al. *Thin Solid Films*[J], 2015, 574: 71
- 15 Wang A N, Huang J H, Hsiao H W et al. *Surface & Coatings Technology*[J], 2015, 280: 43
- 16 Zhu L N, Wang C B, Wang H D et al. *Applied Surface Science*[J], 2012, 258(6): 1944
- 17 Liu Jinna, Xing Zhiguo, Wang Haidou et al. *Vacuum*[J], 2019, 159: 516
- 18 Hamed Masoumi, Seyed Mohsen Safavi, Mehdi Salehi et al. *Materials and Manufacturing Processes*[J], 2014, 29: 1139
- 19 Wang H D, Zhu L N, Xing Z G. *The Detection Technology for Surface Residual Stress*[M]. Beijing: China Machine Press, 2013 (in Chinese)
- 20 Vrbka M, rupka I K, Šamáněk O et al. *Meccanica*[J], 2011, 46: 491
- 21 Kamegawa Takashi, Masuda Yuki, Suzuki Norihiko et al. *ACS Applied Materials and Interfaces*[J], 2011, 3(12): 4561

钛薄膜力学行为和疲劳性能的纳米级动态力学分析

刘金娜^{1,2}, 王海斗², 邢志国², 徐滨士², 崔秀芳¹, 金 国¹

(1. 哈尔滨工程大学, 黑龙江 哈尔滨 150001)

(2. 陆军装甲兵学院 装备再制造技术国防科技重点实验室, 北京 100072)

摘 要: 利用纳米压痕试验研究了不同厚度钛薄膜的力学行为和疲劳性能。在纳米级动态力学分析的基础上, 根据储存刚度的变化定量计算了薄膜的疲劳寿命。结果表明, 薄膜的疲劳寿命与残余应力有显著的关系。压痕原位扫描图像显示, 薄膜出现明显堆积分层, 长裂纹从压头中心向压头边缘垂直延伸。而且, 压痕周围积累了大量的应力, 纳米级动态加载过程产生了高度局域化的塑性变形和应力释放。薄膜内部的残余压应力将抵消部分载荷应力, 提高薄膜的疲劳寿命。

关键词: 钛薄膜; 疲劳; 纳米压痕; 纳米级动态力学分析; 残余应力

作者简介: 刘金娜, 女, 1988 年生, 博士, 讲师, 哈尔滨工程大学材料科学与化学工程学院, 黑龙江 哈尔滨 150001, 电话: 0451-82589056, E-mail: liujinna@hrbeu.edu.cn